

Appendix A

Dispersion Relation of Two-Port Networks

Consider an infinite structure composed of a cascade of identical two-port networks. Using an order-2 transmission ($ABCD$) matrix, we can relate the voltages and currents on either side of the unit cells, as illustrated in Fig. A.1, by

$$\begin{pmatrix} V_L \\ I_L \end{pmatrix} = \begin{pmatrix} A & B \\ C & D \end{pmatrix} \begin{pmatrix} V_R \\ I_R \end{pmatrix}. \tag{A.1}$$

For an infinite periodic structure, the variables on the right can differ from the variables on the left only by the propagation factor, $e^{\gamma l}$, where $\gamma = \alpha + j\beta$ is the complex propagation constant (α and β being the attenuation and phase constants, respectively) and l is the unit-cell length (βl being the electrical length). Accordingly, the above matrix equation can be written as [1, 2]

$$\begin{pmatrix} V_L \\ I_L \end{pmatrix} = \begin{pmatrix} A & B \\ C & D \end{pmatrix} \begin{pmatrix} V_R \\ I_R \end{pmatrix} = \begin{pmatrix} V_R \\ I_R \end{pmatrix} e^{\gamma l}. \tag{A.2}$$

The solution for the propagation constant is given by

$$\left(\begin{pmatrix} A & B \\ C & D \end{pmatrix} - I e^{\gamma l} \right) \begin{pmatrix} V_R \\ I_R \end{pmatrix} = \begin{pmatrix} A - e^{\gamma l} & B \\ C & D - e^{\gamma l} \end{pmatrix} \begin{pmatrix} V_R \\ I_R \end{pmatrix} = 0, \tag{A.3}$$

where I is the identity matrix. For a non-trivial solution

$$\det \begin{pmatrix} A - e^{\gamma l} & B \\ C & D - e^{\gamma l} \end{pmatrix} = 0, \tag{A.4}$$

which yields

$$\cosh(\gamma l) = \frac{A + D}{2}. \tag{A.5}$$

Fig. A.1 Two-port network characterization by the $ABCD$ matrix



For lossless networks and propagating modes ($\alpha = 0$), we can replace $\cosh(\gamma l)$ with $\cos(\beta l)$, and hence the dispersion relation can be rewritten as

$$\cos(\beta l) = \frac{A + D}{2}. \quad (\text{A.6})$$

In addition, for a symmetric network with regard to the ports, $A = D$, so that the solution reduces to

$$\cos(\beta l) = A. \quad (\text{A.7})$$

References

1. D.M. Pozar, *Microwave Engineering*, 3rd edn. (Wiley, New York, 2005)
2. C. Caloz, T. Itoh, *Electromagnetic Metamaterials: Transmission Line Theory and Microwave Applications* (Wiley, New York, 2005)

Appendix B

Equivalent Circuit Models of Electric and Magnetic Couplings

B.1 Electric Coupling

Figure B.1a shows a lumped-element equivalent circuit model for a pair of capacitors, C_1 and C_2 , which are coupled through a mutual capacitance C_m . The electric coupling coefficient is defined as [1, 2]

$$k_e = \frac{C_m}{\sqrt{C_1 C_2}}. \quad (\text{B.1})$$

In the frequency domain, for sinusoidal time-dependence signals, the currents and voltages at the ports are related by

$$I_1 = j\omega C_1 V_1 - j\omega C_m V_2, \quad (\text{B.2a})$$

$$I_2 = j\omega C_2 V_2 - j\omega C_m V_1. \quad (\text{B.2b})$$

By connecting the lower terminals of the circuit model to form a three-terminal network, an equivalent π -circuit composed of only capacitances can be obtained, as depicted in Fig. B.1b [1, 2]. Accordingly, electric coupling is usually modeled by a capacitor connecting the coupled elements.

B.2 Magnetic Coupling

Figure B.2a illustrates a lumped-element equivalent circuit model of two inductors, L_1 and L_2 , coupled by the mutual inductance L_m . The magnetic coupling coefficient is expressed as [1, 2]

$$k_m = \frac{L_m}{\sqrt{L_1 L_2}}. \quad (\text{B.3})$$

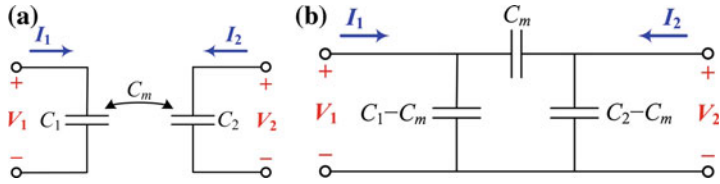


Fig. B.1 **a** Equivalent circuit model of capacitive coupling between two capacitors through a mutual capacitance and **b** transformed equivalent π -circuit

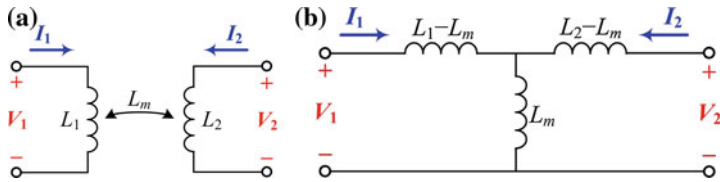


Fig. B.2 **a** Equivalent circuit model of inductive coupling between two inductors by a mutual inductance and **b** transformed equivalent T-circuit

In time-harmonic regime, the currents and voltages at the ports are given by

$$V_1 = j\omega L_1 I_1 + j\omega L_m I_2, \tag{B.4a}$$

$$V_2 = j\omega L_2 I_2 + j\omega L_m I_1. \tag{B.4b}$$

An equivalent T-circuit model can be obtained by connecting the lower terminals, as shown in Fig. B.2b [1–3].

References

1. J.-S. Hong, M.J. Lancaster, *Microstrip Filters for RF/Microwave Applications* (Wiley, New York, 2001)
2. J. Hong, Couplings of asynchronously tuned coupled microwave resonators. *IEEE Proc. Microw. Antennas Propag.* **147**(5), 354–358 (2000)
3. W. Hayt, J. Kemmerly, S. Durbin, *Engineering Circuit Analysis* (McGraw-Hill, New York, 2011)

Appendix C

Even/Odd-Mode S Parameters

Figure C.1a illustrates a four-port network that is assumed to be symmetric and reciprocal. By applying the *even/odd-mode analysis*, the analysis of symmetric N -port networks is reduced to analyzing two $N/2$ -port networks, namely, the even- and odd-mode networks (we restrict the analysis here to $N = 4$) [1–3].

In this method, two modes of excitation are defined, an even mode (symmetric mode) and an odd mode (antisymmetric mode). An even-mode excitation applies in-phase signals with the same amplitude to symmetrical ports (e.g. 1 and 3). Contrarily, an odd-mode excitation is that where anti-phase signals with the same amplitude are applied. Therefore, the whole network can be bisected along the symmetry plane into two identical halves. As shown in Fig. C.1b, the midplane is replaced with a magnetic wall (open circuit) for the even mode and with an electric wall (short circuit) for odd mode. Two two-port networks, namely, the even- and odd-mode networks, result from each of the halves of the symmetric four-port network (e.g. between ports 1 and 2) where the symmetry plane is replaced with a magnetic wall or an electric wall, respectively. The even- and odd-mode networks are characterized by

$$\mathbf{S}_e = \begin{pmatrix} S_{e11} & S_{e21} \\ S_{e21} & S_{e22} \end{pmatrix}, \tag{C.1a}$$

$$\mathbf{S}_o = \begin{pmatrix} S_{o11} & S_{o21} \\ S_{o21} & S_{o22} \end{pmatrix}, \tag{C.1b}$$

where \mathbf{S}_e and \mathbf{S}_o denote the even- and odd-mode scattering (S) matrices, respectively.

As is well known, an arbitrary excitation can be treated as a superposition of appropriate amplitudes of even and odd modes. Consequently, the order-4 S matrix of symmetric four-port networks can be obtained in terms of the even- and odd-mode S parameters as follows [1]

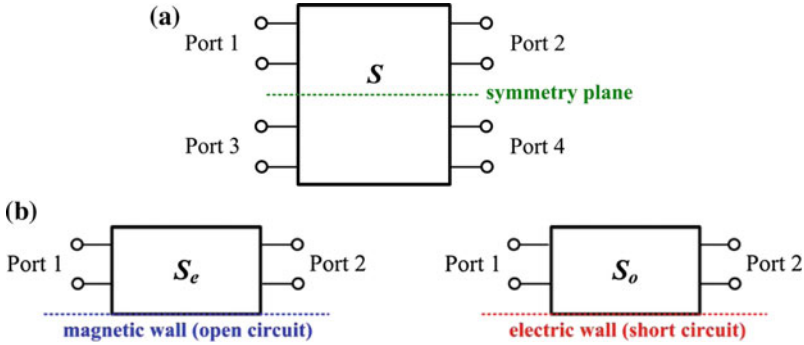


Fig. C.1 **a** Symmetric four-port network characterized by an order-4 S matrix. **b** Two-port even- and odd-mode networks characterized by order-2 S matrices

$$S = \begin{pmatrix} S_{11} & S_{12} & S_{13} & S_{14} \\ S_{21} & S_{22} & S_{23} & S_{24} \\ S_{31} & S_{32} & S_{33} & S_{34} \\ S_{41} & S_{42} & S_{34} & S_{44} \end{pmatrix} = \begin{pmatrix} S_A & S_B \\ S_B & S_A \end{pmatrix}, \quad (\text{C.2})$$

where

$$S_A = \frac{1}{2}(S_e + S_o), \quad (\text{C.3a})$$

$$S_B = \frac{1}{2}(S_e - S_o). \quad (\text{C.3b})$$

Conversely, the S parameters for the even and odd networks can be inferred from the S parameters for the whole network by

$$S_e = S_A + S_B, \quad (\text{C.4a})$$

$$S_o = S_A - S_B. \quad (\text{C.4b})$$

References

1. R.K. Mongia, J. Hong, P. Bhartia, I.J. Bahl, *RF and Microwave Coupled-Line Circuits* (Artech House, Boston, 1999)
2. J.-S. Hong, M.J. Lancaster, *Microstrip Filters for RF/Microwave Applications* (Wiley, New York, 2001)
3. D.M. Pozar, *Microwave Engineering*, 3rd edn. (Wiley, New York, 2005)

Appendix D

Mixed-Mode S Parameters

For the characterization of differential circuits, *mixed-mode scattering (S) parameters* are usually preferred over standard *single-ended S parameters*. Single-ended parameters measure single-ended signals at ports where one of the two terminals is referenced to ground. By contrast, mixed-mode parameters are defined at pairs of single-ended ports, known as *composite* or *mixed-mode ports* [1–3]. Signals at composite ports are decomposed into differential- and common-mode portions, and the simultaneous propagation of such modes is referred to as mixed-mode propagation.

Hence, a differential network may be viewed as a circuit of an even number of N single-ended ports or $N/2$ composite ports (see Fig. D.1). Some vector network analyzers (VNAs) are able to measure directly mixed-mode S parameters. Otherwise, these parameters may be obtained from the measurement of single-ended parameters, and by transformation expressions. For $N = 4$, the mixed-mode parameters defined as [1–3]

$$S_{mm} = \begin{pmatrix} S_{dd} & S_{dc} \\ S_{cd} & S_{cc} \end{pmatrix} = \begin{pmatrix} S_{dd11} & S_{dd12} & S_{dc11} & S_{dc12} \\ S_{dd21} & S_{dd22} & S_{dc21} & S_{dc22} \\ S_{cd11} & S_{cd12} & S_{cc11} & S_{cc12} \\ S_{cd21} & S_{cd22} & S_{cc21} & S_{cc22} \end{pmatrix}, \tag{D.1}$$

can be expressed in terms of the single-ended parameters by

$$S_{dd} = \frac{1}{2} \begin{pmatrix} S_{11} - S_{13} - S_{31} + S_{33} & S_{12} - S_{14} - S_{32} + S_{34} \\ S_{21} - S_{23} - S_{41} + S_{43} & S_{22} - S_{24} - S_{42} + S_{44} \end{pmatrix}, \tag{D.2a}$$

$$S_{cc} = \frac{1}{2} \begin{pmatrix} S_{11} + S_{13} + S_{31} + S_{33} & S_{12} + S_{14} + S_{32} + S_{34} \\ S_{21} + S_{23} + S_{41} + S_{43} & S_{22} + S_{24} + S_{42} + S_{44} \end{pmatrix}, \tag{D.2b}$$

$$S_{cd} = \frac{1}{2} \begin{pmatrix} S_{11} - S_{13} + S_{31} - S_{33} & S_{12} - S_{14} + S_{32} - S_{34} \\ S_{21} - S_{23} + S_{41} - S_{43} & S_{22} - S_{24} + S_{42} - S_{44} \end{pmatrix}, \tag{D.2c}$$

$$S_{dc} = \frac{1}{2} \begin{pmatrix} S_{11} + S_{13} - S_{31} - S_{33} & S_{12} + S_{14} - S_{32} - S_{34} \\ S_{21} + S_{23} - S_{41} - S_{43} & S_{22} + S_{24} - S_{42} - S_{44} \end{pmatrix}. \tag{D.2d}$$

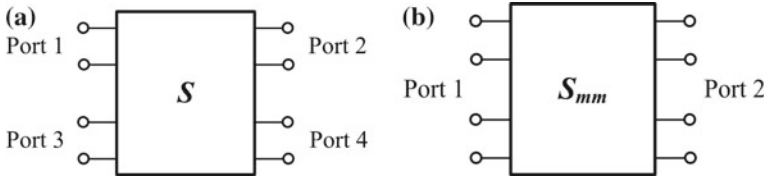


Fig. D.1 Port configuration for the transformation between **a** single-ended and **b** mixed-mode S parameters. The case with $N = 4$ corresponding to **a** four single-ended ports and **b** two composite ports is illustrated

S_{dd} stands for the differential-mode S parameters, S_{cc} represents the common-mode S parameters, and S_{cd} and S_{dc} account for the mode-conversion or cross-mode S parameters.

If the network is symmetric¹ and reciprocal, the cross-mode parameters are zero, whereas the differential- and common-mode parameters are the same as the odd- and even-mode single-ended parameters (Appendix C), i.e.

$$S_{dd} = S_o, \quad (\text{D.3a})$$

$$S_{cc} = S_e. \quad (\text{D.3b})$$

However, it should be highlighted that the reference impedance at the ports for the differential- and common-mode are, respectively,

$$Z_{0dd} = 2Z_0, \quad (\text{D.4a})$$

$$Z_{0cc} = \frac{Z_0}{2}, \quad (\text{D.4b})$$

where Z_0 is the reference impedance to calculate the single-ended S parameters. The previous relationships come from the definition of voltages and currents at the ports (not included in the Appendix). Therefore, if $Z_0 = 50 \Omega$ as usual, the reference impedances to calculate the mixed-mode S parameters become $Z_{0dd} = 100$ and $Z_{0cc} = 25 \Omega$.

References

1. D. Bockelman, W. Eisenstadt, Combined differential and common-mode scattering parameters: theory and simulation. *IEEE Trans. Microw. Theory Tech.* **43**(7), 1530–1539 (1995)
2. W.R. Eisenstadt, *Microwave Differential Circuit Design using Mixed-Mode S-Parameters* (Artech House, Boston, 2006)
3. G.D. Vendelin, A.M. Pavio, U.L. Rohde, *Microwave Circuit Design Using Linear and Nonlinear Techniques* (Wiley, New York, 2005)

¹Ideally, a differential circuit should be perfectly symmetric.

Appendix E

Rejection Bandwidth Definition

This appendix discusses the relation between the stopband bandwidth inferred from the dispersion relation and the -20 dB bandwidth obtained from the S parameters in a network with a significant number of cells. Particularly, the analysis is carried out by using the even-mode equivalent circuit model of a specific CSRR-loaded differential line (see Fig. E.1).

The dispersion relation of the considered network is plotted in Fig. E.2. In the circuit under study, the forbidden band includes the region where complex modes are present (between 1.42 and 1.61 GHz), plus an additional region in which the modes are evanescent (from 1.61 to 1.93 GHz). As is well known, the dispersion relation provides the frequency regions where signal propagation is allowed or forbidden for an infinitely periodic structure. For a finite number of cells, the most relevant effects that may occur are impedance mismatch in the allowed bands or small rejection within the forbidden bands. Therefore, an analysis to determine the rejection level that properly defines the forbidden band in a truncated structure is very convenient.

It is also well known that the transmission coefficient in two-port periodic structures suffers from ripple in the allowed bands. Such ripple is caused by impedance mismatch, and maximum transmission is produced at those frequencies where either the Bloch impedance [1, 2] is matched to the impedance of the ports (impedance matching) or the electrical length is a multiple of π (phase matching). Between adjacent transmission peaks, the transmission coefficient is a minimum at those frequencies where the phase is an odd multiple of $\pi/2$. The transmission coefficient at these frequencies of minimum transmission can be easily obtained according to [3]

$$f_{env}(\omega) = 10 \log_{10} \left\{ 1 - \left| \frac{Z_B^2(\omega) - Z_0^2}{Z_B^2(\omega) + Z_0^2} \right|^2 \right\}, \quad (\text{E.1})$$

where $Z_B(\omega)$ is the Bloch impedance and Z_0 the reference impedance of the ports ($Z_0 = 50 \Omega$). Expression (E.1) corresponds to the envelope of the transmission

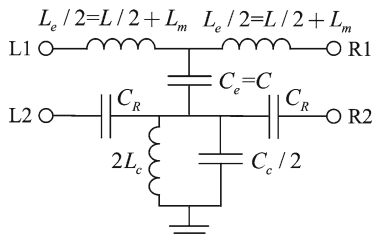


Fig. E.1 Even-mode circuit model (unit cell) of a CSRR-loaded differential line. The considered circuit parameters are: $L_e = 6.3$ nH, $C_e = 1.1$ pF, $L_c = 2.1$ nH, $C_c = 3.2$, and $C_R = 0.1$ pF (those corresponding to the CSRR-based common-mode filter with $f_z = 1.5$ GHz in Table 5.1)

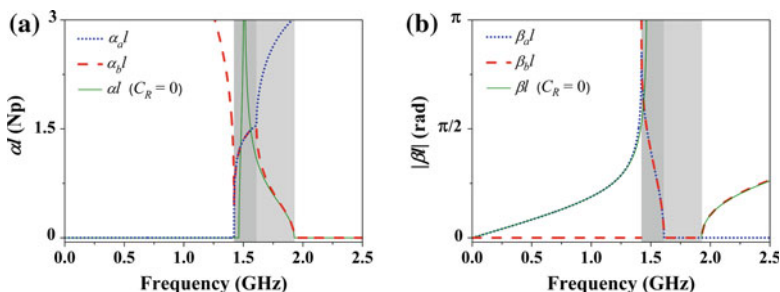


Fig. E.2 **a** Real part and **b** magnitude of the imaginary part of γl corresponding to the two modes of the considered network, where α is the attenuation constant, β the phase constant, and l the elemental cell period. If inter-resonator coupling is canceled ($C_R = 0$), the two modes degenerate into a single mode, also depicted. The evanescent and complex mode regions are highlighted in *light* and *dark gray*, respectively. Reprinted with permission from [5]

coefficient in the allowed bands of a two-port structure. However, the structure under analysis is described by a circuit model with two input and output ports (see Fig. E.1). In a two-port structure, the Bloch impedance is obtained by the ratio between the eigenvector variables (voltage and current). For the circuit under study, the pair of eigenvectors ($[V_{1a}, V_{2a}, I_{1a}, I_{2a}]$ and $[V_{1b}, V_{2b}, I_{1b}, I_{2b}]$ where a and b discriminate each mode) can be obtained by using

$$\begin{pmatrix} V_L \\ I_L \end{pmatrix} = \begin{pmatrix} A & B \\ C & D \end{pmatrix} \begin{pmatrix} V_R \\ I_R \end{pmatrix}, \quad (\text{E.2})$$

and,

$$\cosh(\gamma l) = \frac{1}{2} \left(A_{11} + A_{22} \pm \sqrt{(A_{11} - A_{22})^2 + 4A_{12}A_{21}} \right), \quad (\text{E.3})$$

and we can infer from them the characteristic impedance matrix as follows [4]

$$\mathbf{Z}_c = \mathbf{V}_{ab} \cdot \mathbf{I}_{ab}^{-1}, \quad (\text{E.4})$$

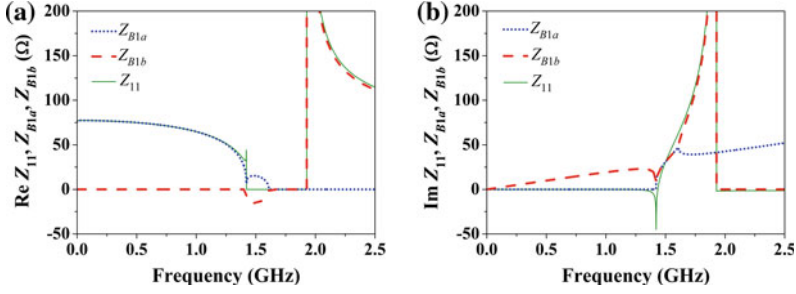


Fig. E.3 a Real and b imaginary part of Z_{11} , Z_{B1a} , and Z_{B1b} . Reprinted with permission from [5]

where V_{ab} and I_{ab} are 2×2 matrices formed by column vectors composed of the eigenvector voltages and currents

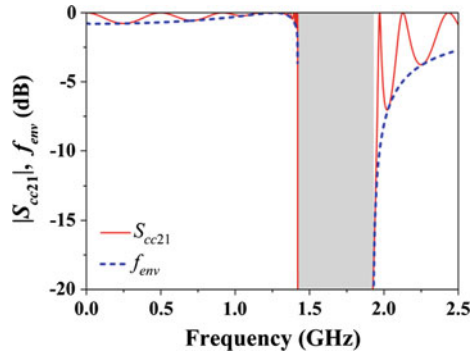
$$V_{ab} = \begin{pmatrix} V_{1a} & V_{1b} \\ V_{2a} & V_{2b} \end{pmatrix}, \quad (\text{E.5a})$$

$$I_{ab} = \begin{pmatrix} I_{1a} & I_{1b} \\ I_{2a} & I_{2b} \end{pmatrix}. \quad (\text{E.5b})$$

The diagonal elements of Z_c (Z_{11} and Z_{22}) are simply the ratios between the voltage and current in the corresponding port when the other port is left open-circuited, whereas the anti-diagonal elements determine the effects of the current injected into one port on the voltage in the other port when it is opened. Note that Z_{11} and Z_{22} are not the ratios of the voltage and current at ports 1 and 2 for each eigenvector. Let us denote such voltage to current ratios for port 1 by Z_{B1a} and Z_{B1b} . If we now compare Z_{11} to Z_{B1a} and Z_{B1b} (Fig. E.3), it can be appreciated that $Z_{11} \approx Z_{B1a}$ on the left of the forbidden band, whereas $Z_{11} \approx Z_{B1b}$ on the right of that band. This means that, in the allowed bands, the propagation in an infinite structure resulting by cascading the networks of Fig. E.1 with port L2 of the first cell left opened, can be described as if it was a two-port network that supports the eigenvector composed of the variables referred to port 1 (mode a and b on the left and right of the stop band, respectively) and Bloch impedance given by Z_{11} . This approximation is valid as long as mode mixing is negligible, as occurs in the whole allowed frequency region except in a narrow band on the left of the stop band, where modes a and b co-exist (this leads to a complex value of Z_{11} in that region).

From the previous statements, it follows that the envelope function of the transmission coefficient of any finite structure with ports L2 and R2 of the first and last cell, respectively, left open-circuited (actual conditions), can be approximated by means of (E.1), considering $Z_B = Z_{11}$. The envelope function in the allowed bands inferred through (E.1) with Z_{11} is compared to the response of a 12-cell structure

Fig. E.4 Transmission coefficient of the 12-cell structure resulting by cascading the 4-port network of Fig. E.1 with L2 and R2 ports of stages 1 and 12, respectively, left opened, and envelope function in the allowed bands. The forbidden band is depicted in gray. Reprinted with permission from [5]



in Fig. E.4. It is confirmed that we can use expression (E.1) to obtain the envelope function to a very good approximation.²

With regard to the stopband bandwidth, it coincides with the region delimited by those frequencies where the envelope function exhibits a vertical slope. This vertical slope is clearly achieved at a rejection level of 20 dB. In view of this result, the 20-dB rejection level is intimately related to the stopband bandwidth obtained by the dispersion relation, and is a good rejection level to define the common-mode rejection bandwidth.

References

1. D.M. Pozar, *Microwave Engineering*, 3rd edn. (Wiley, New York, 2005)
2. F. Martín, *Artificial Transmission Lines for RF and Microwave Applications* (Wiley, New York, 2015)
3. M. Gil, J. Bonache, I. Gil, J. García-García, F. Martín, On the transmission properties of left-handed microstrip lines implemented by complementary split rings resonators. *Int. J. Numer. Model. Electron. Networks Devices Fields* **19**(2), 87–103 (2006)
4. R.K. Mongia, J. Hong, P. Bhartia, I.J. Bahl, *RF and Microwave Coupled-Line Circuits* (Artech House, Boston, 1999)
5. J. Naqui, A. Fernández-Prieto, M. Durán-Sindreu, F. Mesa, J. Martel, F. Medina, F. Martín, Common-mode suppression in microstrip differential lines by means of complementary split ring resonators: theory and applications. *IEEE Trans. Microw. Theory Tech.* **60**(10), 3023–3034 (2012)

²It should be emphasized that the proposed procedure to infer the envelope function is approximate. However, expression (E.1) provides very good results because the coupling capacitance between resonators, C_R , is small in the considered structures. If this condition is not fulfilled, mode mixing is more pronounced, and the envelope function that results when the ports L2 and R2 of the input and output cells, respectively, are opened, cannot be inferred following this simple procedure.

Appendix F

Envelope Detector Design

An envelope detector as that depicted in Fig. 6.25a works on a charging-discharging scheme [1]. Assuming an ideal diode, in the positive half-cycle of the modulated signal, the diode is forward-biased and the capacitor C charges rapidly to the peak value of the modulated signal with a time constant

$$\tau_c = Z_0 C \ll T_c, \tag{F.1}$$

where $T_c = 1/f_c$ is the period of the carrier signal. When the input signal falls below the peak value, the diode becomes reverse-biased, and the capacitor discharges slowly through the load resistor R until the next positive half-cycle, with a time constant, τ_d , satisfying

$$T_c \ll \tau_d = RC \ll T_m. \tag{F.2}$$

In the readout circuit in Fig. 6.25a, at the detector output, the envelope signal in time domain can be visualized by an oscilloscope. The waveform of the envelope is directly related to the transfer function (ideally they should be identical). Ideally, the input impedance of an oscilloscope should be infinite. However, in practice, loading effects arise (the input impedance is finite and complex, with resistive and capacitive components in parallel). Thus, for low loading effects, high resistance and low capacitance are required. For the available oscilloscope the input impedance is $1\text{ M}\Omega$ in parallel with 14 pF [2]. Regardless of the value of C , the input capacitance of the oscilloscope is not small enough, and condition (F.1) cannot be satisfied. Nevertheless, note that the input impedance of the oscilloscope is indeed an RC filter as that of the detector circuit. Therefore, we may take advantage of the loading effects to inherently implement the filter with the measurement. However, as mentioned before, the input capacitance is not small enough. For this reason, a single-ended active probe is used, achieving an input impedance of $1\text{ M}\Omega$ in parallel with 1 pF . Thereby conditions (F.1) and (F.2) are satisfied. For the sensor in Fig. 6.24, the conditions yield

$$T_c/\tau_c = 13.2 \gg 1, \quad (\text{F.3a})$$

$$T_m/\tau_d = 5 \cdot 10^5 (60 \text{ rpm}) \gg 1, \quad (\text{F.3b})$$

$$T_m/\tau_d = 10^4 (3,000 \text{ rpm}) \gg 1, \quad (\text{F.3c})$$

$$\tau_d/T_c = 1.52 \cdot 10^3 \gg 1. \quad (\text{F.3d})$$

References

1. S. Haykin, *Communication Systems* (Wiley, New York, 2001)
2. J. Naqui, F. Martín, Transmission lines loaded with bisymmetric resonators and their application to angular displacement and velocity sensors. *IEEE Trans. Microw. Theory Tech.* **61**(12), 4700–4713 (2013)